nanomaterials

Article

A Facile Strategy for the Preparation of N-Doped TiO_2 with Oxygen Vacancy via the Annealing Treatment with Urea

Zhe Zhang [1], Zhenpeng Cui [1,2,*], Yinghao Xu [1], Mohamed Nawfal Ghazzal [3], Christophe Colbeau-Justin [3], Duoqiang Pan [1,2] and Wangsuo Wu [1,2]

1 School of Nuclear Science and Technology, Lanzhou University, Lanzhou 730000, China
2 Frontiers Science Center for Rare Isotopes, Lanzhou University, Lanzhou 730000, China
3 Institute of Physical Chemistry, Paris-Saclay University, 91405 Orsay, France
* Correspondence: cuizp@lzu.edu.cn

Abstract: Although titanium dioxide (TiO_2) has a wide range of potential applications, the photocatalytic performance of TiO_2 is limited by both its limited photoresponse range and fast recombination of the photogenerated charge carriers. In this work, the preparation of nitrogen (N)-doped TiO_2 accompanied by the introduction of oxygen vacancy (Vo) has been achieved via a facile annealing treatment with urea as the N source. During the annealing treatment, the presence of urea not only realizes the N-doping of TiO_2 but also creates Vo in N-doped TiO_2 (N-TiO_2), which is also suitable for commercial TiO_2 (P25). Unexpectedly, the annealing treatment-induced decrease in the specific surface area of N-TiO_2 is inhibited by the N-doping and, thus, more active sites are maintained. Therefore, both the N-doping and formation of Vo as well as the increased active sites contribute to the excellent photocatalytic performance of N-TiO_2 under visible light irradiation. Our work offers a facile strategy for the preparation of N-TiO_2 with Vo via the annealing treatment with urea.

Keywords: nitrogen doping; TiO_2; oxygen vacancy; annealing treatment; urea

check for updates

Citation: Zhang, Z.; Cui, Z.; Xu, Y.; Ghazzal, M.N.; Colbeau-Justin, C.; Pan, D.; Wu, W. A Facile Strategy for the Preparation of N-Doped TiO_2 with Oxygen Vacancy via the Annealing Treatment with Urea. *Nanomaterials* **2024**, *14*, 818. https://doi.org/10.3390/nano14100818

Academic Editor: Alexandra Carvalho

Received: 3 April 2024
Revised: 29 April 2024
Accepted: 2 May 2024
Published: 7 May 2024

1. Introduction

Titanium dioxide (TiO_2) has been widely investigated because of its excellent chemical stability, nontoxicity, and low cost [1,2]. Although TiO_2 shows great potential in many fields [3–5], it can only absorb ultraviolet (UV) light [6], which limits its sufficient absorption of solar light because visible light (43%) takes up the majority of the solar spectrum [7]. In addition, the fast recombination of photogenerated charge carriers in TiO_2 impedes its efficient use of solar energy [8,9]. Thus, in order to improve the photocatalytic performance of TiO_2, not only does the photoresponse range need to be extended but also the recombination of photogenerated charge carriers needs to be inhibited [10,11].

To extend the photoresponse range of TiO_2 from UV light to visible light, the doping strategy is commonly applied to adjust the intrinsic wide bandgap of TiO_2 [12,13]. Among various doping strategies, it is reported that nitrogen (N) doping is an effective approach to reduce the bandgap of TiO_2 and enables its absorption of visible light [14–16]. Generally, the preparation of N-doped TiO_2 can be realized by the annealing treatment with the presence of additional N sources such as urea and ammonia [17–19]. To reduce the recombination of photogenerated charge carriers, the formation of defective structure is reported to be a useful strategy [6,20]. The introduction of point defects into TiO_2, such as oxygen vacancy (Vo), could trap the photogenerated electron inhibiting the recombination of the photogenerated charge carriers [10,21]. Although many methods have been reported for the creation of Vo in TiO_2 [22–24], the annealing treatment of TiO_2 with an organic additive is reported to be an easy approach for the creation of Vo [25,26]. Thus, it is of great interest to realize both the N-doping and creation of Vo to enhance the photocatalytic performance of TiO_2.

To realize both the N-doping and introduction of Vo in one step, in this work, a facile strategy has been developed to prepare N-doped TiO_2 accompanied by the formation of Vo via the annealing treatment with urea. The effects of the annealing treatment on the photoresponse property and crystal structure of TiO_2 have been investigated as a function of the amount of urea. The photocatalytic performance of as-synthesized TiO_2 photocatalysts has been evaluated by the photocatalytic degradation of organic pollutants under visible light irradiation.

2. Materials and Methods

2.1. Materials

Hydrothermally prepared TiO_2 was obtained according to the reported synthetic procedures [27]. Commercially available TiO_2 (P25, Degussa, Evonik, Resource Effiency GmbH, Essen, Germany) was purchased and used without further treatment. Custom-built high-borosilicate glass tubes were used for the annealing treatment. Methyl orange (MO, AR grade, Beijing Chemical Plant Co., Beijing City, China) was chosen as the model organic pollutant for evaluating the photocatalytic performance of all photocatalysts.

2.2. Annealing Treatment

To prepare the N-doped TiO_2 via the annealing treatment, both hydrothermally prepared TiO_2 and urea were sealed in high-borosilicate glass tubes under vacuum and annealed at 500 °C for 2 h. The amount of TiO_2 (100 mg) was kept the same and the weight ratios of TiO_2 to urea were set as 1:0, 2:1, 1:1, and 1:2 (Figure S1). The obtained samples were named as A-TiO_2, N-TiO_2 (2:1), N-TiO_2 (1:1), and N-TiO_2 (1:2), respectively. Similarly, the annealing treatment of P25 with urea was conducted under the same conditions (Figure S2). The obtained samples were abbreviated as A-P25, N-P25 (2:1), N-P25 (1:1), and N-P25 (1:2), respectively (Figure S3). For comparison purposes, the annealing treatment of urea (100 mg) was also performed under the same conditions (Figures S4 and S5). All the as-synthesized samples were collected for further characterizations and tests.

2.3. Characterizations

The diffuse reflectance spectra (DRS) were measured by the UV-vis diffuse reflectance spectroscopy (UV-2600, Shimadzu, Kyoto, Japan). The diffraction patterns were recorded by X-ray diffraction (XRD, Ultima IV, Rigaku, Tokyo, Japan) with a Cu-Kα radiation source (λ = 1.5406 Å). Brunauer–Emmett–Teller (BET) surface areas were determined with an accelerated surface area and porosity analyzer (ASAP 2460, Micrometrics, Norcross, GA, USA). Electron paramagnetic resonance (EPR, ER200DSRC, Bruker, Mannheim, Germany) spectra were taken by applying an X-band (9.44 GHz, 2.47 mW) microwave and sweeping magnetic field at room temperature. The ultraviolet-visible (UV-vis) spectra were obtained with a UV-vis spectrophotometer (Lambda 35, PerkinElmer, Waltham, MA, USA).

2.4. Photocatalytic Performance

Photocatalytic degradation of MO was carried out under visible light irradiation (Xenon lamp, 300 W, PerfectLight, Beijing, China) with a long-wavelength pass filter (>420 nm). TiO_2 photocatalysts (25 mg, 1 mg/mL) were added to aqueous solutions of MO (25 ppm, 25 mL) and stirred in dark for 60 min. The concentration variation of MO as a function of irradiation time was monitored by measuring its characteristic peak centered at 464 nm. The photocatalytic degradation ratio of MO was estimated by the expression: $(C_0 - C)/C_0 \times 100\%$, where C_0 is the initial concentration of MO and C corresponds to the concentration of MO at different time intervals.

3. Results and Discussion

3.1. Characterizations of TiO_2 Photocatalysts

As shown in Figure 1, hydrothermally prepared TiO_2 appears as a white powder before the annealing treatment (Figure 1a and Figure S1a). In the absence of urea, TiO_2

turns to a dark grey powder after the annealing treatment (Figure 1b and Figure S1e) due to the pyrolysis of the organic solvent [27,28]. With the presence of urea (Figure S1b–d), TiO_2 is transformed to a brown powder after the annealing treatment (Figure S1f–h). This obvious color change indicates that N-doping of TiO_2 may happen during the annealing treatment with urea as the N source [29,30]. Although the amount of urea increases, the colors of all N-TiO_2 samples are similar, implying that a low amount of urea is enough for N-doping (Figure 1c–e). This facile strategy is also suitable for the preparation of N-doped P25 (Figure S2) and white P25 changes to a brown powder after the annealing treatment with urea (Figure S3). Since the annealing treatment results in no clear color change of urea (Figures S4 and S5), it is reasonable to propose that the pyrolysis of urea leads to the N-doping of TiO_2 during the annealing treatment.

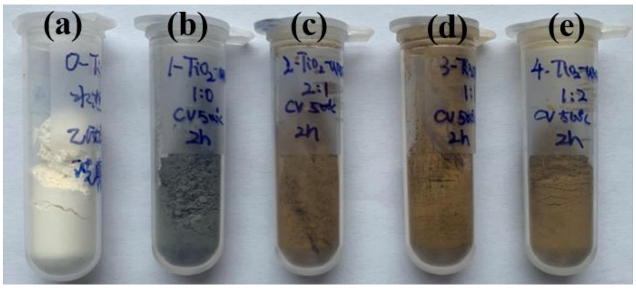

Figure 1. Digital photographs of (**a**) TiO_2, (**b**) A-TiO_2, (**c**) N-TiO_2 (2:1), (**d**) N-TiO_2 (1:1), and (**e**) N-TiO_2 (1:2).

To investigate the effects of the annealing treatment on the photoresponse property of TiO_2, the DRS spectra of all samples were recorded. According to Figure 2a, both TiO_2 and A-TiO_2 show clear UV absorption and a negligible visible light response. This result is in agreement with the color of TiO_2 and the reported phenomenon [27]. Conversely, all N-TiO_2 samples present obvious visible light absorption with almost identical absorbance, which further proves that a low amount of urea is enough for N-doping. The annealing treatment of TiO_2 with urea definitely expands the photoresponse range of TiO_2 to the visible light range suggesting that N-doping occurs [13,31]. To further confirm the N-doping of TiO_2, N1s XPS fine spectra of all samples were collected. Compared with TiO_2 and A-TiO_2, all N-TiO_2 samples show a clear N1s peak which undoubtedly proves that the N-doping of TiO_2 occurs [32,33]. In addition, the peak intensity increases as the amount of urea goes up, implying an increase in the N-doping level [18,34]. Thus, the annealing treatment of urea offers a facile approach for the preparation of N-doped TiO_2 to extend the photoresponse range of TiO_2.

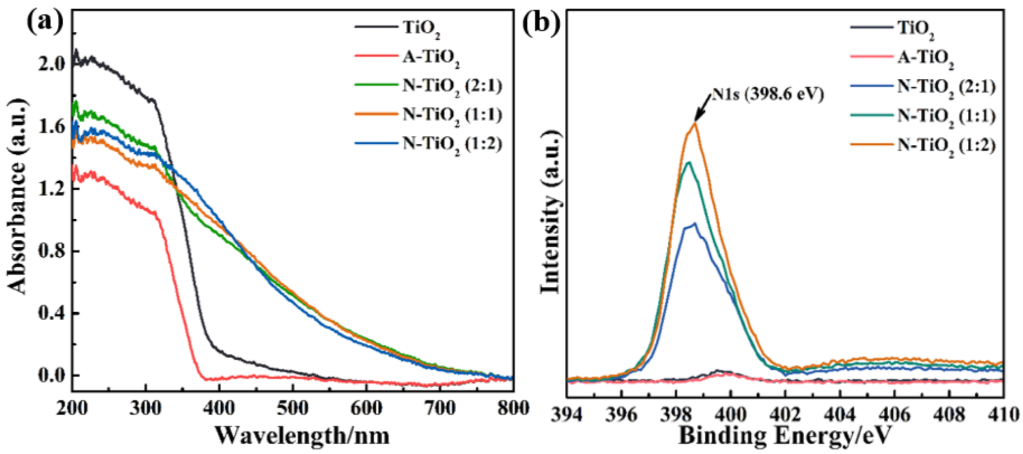

Figure 2. (**a**) DRS spectra and (**b**) N1s XPS fine spectra of TiO_2, A-TiO_2, N-TiO_2 (2:1), N-TiO_2 (1:1), and N-TiO_2 (1:2).

To further study the influences of the annealing treatment on the crystal structures of TiO_2, XRD measurements were conducted and the results are shown in Figure 3. All the characteristic diffraction patterns of TiO_2 photocatalysts are in accordance with the diffraction peaks of anatase, proving that the crystal phase of all TiO_2 samples is anatase (JCPDS-21-1272) [25,35]. In the absence of urea, the crystallinity of TiO_2 is improved after the annealing treatment as indicated by the increased intensity of the diffraction patterns which correspond to the (101) and (200) crystal planes. However, the crystallinity of all N-TiO_2 samples is similar to that of TiO_2 after the annealing treatment with urea. This unexpected phenomenon suggests that N-doping hampers the further crystallization of N-TiO_2 which may enlarge its specific surface area [3,36]. In addition, new diffraction patterns appear close to the (101) crystal plane of N-TiO_2 (1:2), suggesting that a low amount of urea is enough for the N-doping.

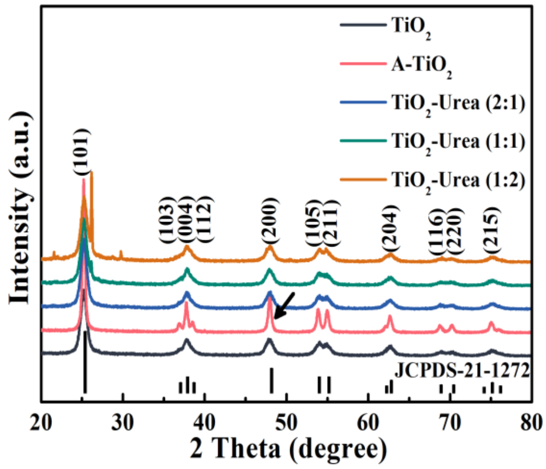

Figure 3. XRD patterns of TiO_2, A-TiO_2, N-TiO_2 (2:1), N-TiO_2 (1:1), and N-TiO_2 (1:2). The arrow shows the (200) diffraction peak of A-TiO_2 [25].

The BET surface areas of all samples were measured to further analyze the effect of the annealing treatment on TiO_2. From Table 1, it is clear that the BET surface area of hydrothermally prepared TiO_2 (134.67 m^2/g) is the largest whereas that of A-TiO_2 is the smallest (40.21 m^2/g). Compared with TiO_2, the specific surface areas of N-TiO_2 samples decrease and a decreasing tendency is observed as the amount of urea increases. Clearly, the annealing treatment of TiO_2 with urea inhibits its crystallization which is in agreement with the results of XRD (Figure 3). For the moment, the reason for this phenomenon has been reported and it may result from the N-doping induced by the annealing treatment [3]. This phenomenon is also observed in the P25 samples obtained after the annealing treatment with urea (Table S1). As a result, the annealing treatment with urea offers a facile approach for the preparation of N-doped TiO_2 with more active sites reserved.

Table 1. BET surface area of TiO_2, A-TiO_2, N-TiO_2 (2:1), N-TiO_2 (1:1), and N-TiO_2 (1:2).

Sample	BET (m^2/g)
TiO_2	134.67
A-TiO_2	40.21
N-TiO_2 (2:1)	107.59
N-TiO_2 (1:1)	73.36
N-TiO_2 (1:1)	51.87

To further investigate the influences of the annealing treatment on the crystal structure of TiO_2, EPR spectra of all samples were recorded and are shown in Figure 4. As shown in Figure 4, the characteristic peak with a g value of 2.002 corresponds to Vo [20,37]. Compared with TiO_2, A-TiO_2 contains a certain amount of Vo which may result from the both the crystallization of TiO_2 and the pyrolysis of the organic solvents [25,26]. With the presence of urea, more Vo is introduced into the N-doped TiO_2 and its amount increases first and then decreases as the amount of urea increases. This result may be due to the N-doping process which not only induces the formation of Vo but can also occupy the Vo. The formation of Vo in N-doped TiO_2 may contribute to the separation of photogenerated charge carriers [38,39]. Thus, the annealing treatment with urea not only induces the N-doping to extend the photoresponse range of TiO_2 but also creates Vo in N-doped TiO_2 which contributes to the separation of photogenerated charge carriers, which could both favor the enhancement of the photocatalytic performance of TiO_2.

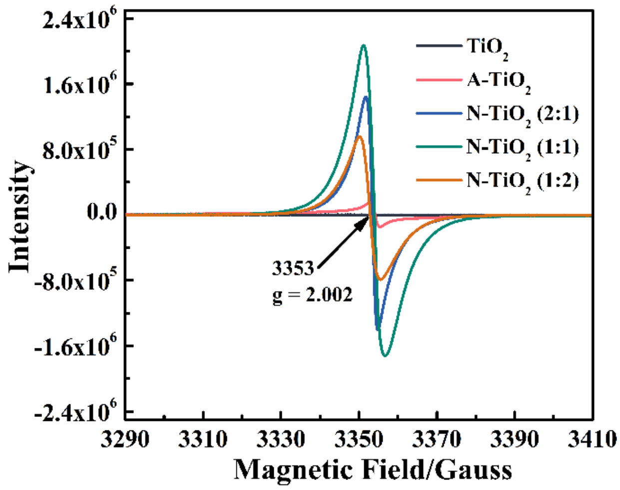

Figure 4. EPR spectra of TiO_2, $ATiO_2$, N-TiO_2 (2:1), N-TiO_2 (1:1), and N-TiO_2 (1:2).

3.2. Photocatalytic Performance

The photocatalytic performance of all TiO_2 photocatalysts was evaluated by the photocatalytic degradation of MO under visible light irradiation. From Figure 5, all TiO_2 photocatalysts are capable of adsorbing a certain amount of MO and N-TiO_2 (1:2) shows (1:1) the highest adsorption capacity for MO (12.9%). Compared with TiO_2, the specific surface area of N-TiO_2 (1:2) is smaller and its improved adsorption capacity of MO may be due to the formation of functional groups, which is in agreement with the XRD analysis (Figure 3). During visible light irradiation, both TiO_2 and A-TiO_2 are not able to degrade MO because they do not absorb the visible light (Figure 2a). With N-TiO_2 as the photocatalyst, the photocatalytic degradation of MO is feasible and among the samples N-TiO_2 (2:1) presents the best photocatalytic performance. The photocatalytic performance of N-TiO_2 proves that the annealing treatment with urea extends the photoresponse range of TiO_2 to the visible light range [18,40]. The photocatalytic performance of N-TiO_2 is comparable to the reported results (Table S2) which may be ascribed to the formation of Vo and the increased specific surface area [33,39,41,42]. Based on the photocatalytic performance, the optimal weight ratio of TiO_2 to urea for the preparation of N-TiO_2 via the annealing treatment is found to be 2:1.

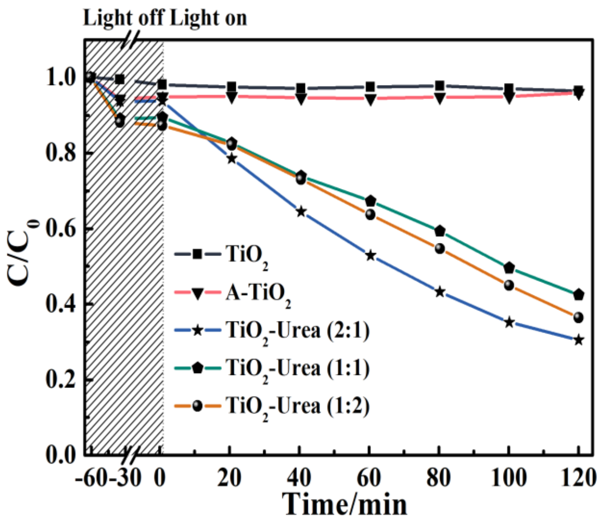

Figure 5. Photocatalytic degradation curves of MO by TiO_2, A-TiO_2, N-TiO_2 (2:1), N-TiO_2 (1:1), and N-TiO_2 (1:2) under visible light irradiation.

4. Conclusions

In summary, a facile strategy was developed for the preparation of N-TiO_2 via the annealing treatment with urea. On the one hand, the photoresponse of TiO_2 is extended by N-doping via the annealing treatment with urea as the N source. On the other hand, Vo is introduced into N-TiO_2 which may contribute to the separation of photogenerated charge carriers. In addition, the specific surface area of N-TiO_2 is enlarged with the presence of urea during the annealing treatment by inhibiting the crystallization of TiO_2. Thus, more active sites could be reserved for photocatalytic reactions. All the above favorable aspects induced by the annealing treatment with urea contribute to the excellent photocatalytic performance of N-TiO_2. This facile strategy is also suitable for other TiO_2 photocatalysts such as P25 and, thus, our work offers a universal approach for the preparation of N-doped TiO_2 via the annealing treatment with urea. The annealing treatment with other additives for different elements doping, not merely N doping, may be also possible and further work is underway.

Supplementary Materials: The following supporting information can be downloaded at: https://www.mdpi.com/article/10.3390/nano14100818/s1, Figure S1: Digital photographs of TiO_2 and urea (a–d) before and (e–h) after the annealing treatment (500 °C, 2 h). The weight ratios of TiO_2 to urea are (a,e) 1:0, (b,f) 2:1, (c,g) 1:1 and (d,h) 1:2, respectively. Figure S2: Digital photographs of P25 and urea (a–d) before and (e–h) after the annealing treatment (500 °C, 2 h). The weight ratios of P25 to urea are (a,e) 1:0, (b,f) 2:1, (c,g) 1:1 and (d,h) 1:2, respectively. Figure S3: Digital photographs of (a) P25, (b) A-P25, (c) N-P25 (2:1), (d) N-P25 (1:1), and (e) N-P25 (1:2). Figure S4: Digital photographs of urea (a) before and (b) after the annealing treatment (500 °C, 2 h). Figure S5: Digital photographs of the urea (a) before and (b) after the annealing treatment (500 °C, 2 h). Table S1: BET surface area of P25, A-P25, N-P25 (2:1), N-P25 (1:1), and N-P25 (1:2). Table S2: Comparison of photocatalytic activity of N-TiO_2 photocatalyst for degradation of MO [43–49].

Author Contributions: Z.Z.: investigation, visualization, formal analysis, and writing—original draft. Y.X.: validation, formal analysis, and investigation. M.N.G.: validation and data curation. C.C.-J.: validation, formal analysis and data curation. D.P.: validation and formal analysis. W.W.: validation and formal analysis. Z.C.: conceptualization, project administration, supervision, resources, writing—review and editing and funding acquisition. All authors have read and agreed to the published version of the manuscript.

Funding: This work was supported by the National Natural Science Foundation of China (No. 12005086).

Data Availability Statement: Data will be made available on request.

Acknowledgments: The authors acknowledge the China Scholarship Council (CSC) for the financial support.

Conflicts of Interest: The authors declare that they have no known competing financial interests or personal relationships that could have appeared to influence the work reported in this paper.

References

1. Schneider, J.; Matsuoka, M.; Takeuchi, M.; Zhang, J.; Horiuchi, Y.; Anpo, M.; Bahnemann, D.W. Understanding TiO_2 photocatalysis: Mechanisms and materials. *Chem. Rev.* **2014**, *114*, 9919–9986. [CrossRef]
2. Ma, Y.; Wang, X.L.; Jia, Y.S.; Chen, X.B.; Han, H.X.; Li, C. Titanium Dioxide-Based Nanomaterials for Photocatalytic Fuel Generations. *Chem. Rev.* **2014**, *114*, 9987–10043. [CrossRef] [PubMed]
3. Zhou, Y.; Liu, Y.; Liu, P.; Zhang, W.; Xing, M.; Zhang, J. A facile approach to further improve the substitution of nitrogen into reduced TiO_{2-x} with an enhanced photocatalytic activity. *Appl. Catal. B Environ.* **2015**, *170–171*, 66–73. [CrossRef]
4. Wang, C.; Li, J.; Paineau, E.; Laachachi, A.; Colbeau-Justin, C.; Remita, H.; Ghazzal, M.N. A sol-gel biotemplating route with cellulose nanocrystals to design a photocatalyst for improving hydrogen generation. *J. Mater. Chem. A* **2020**, *8*, 10779–10786. [CrossRef]
5. Wang, W.; Tadé, M.; Shao, Z. Nitrogen-doped simple and complex oxides for photocatalysis: A review. *Prog. Mater. Sci.* **2018**, *92*, 33–63. [CrossRef]
6. Naldoni, A.; Altomare, M.; Zoppellaro, G.; Liu, N.; Kment, Š.; Zbořil, R.; Schmuki, P. Photocatalysis with Reduced TiO_2: From Black TiO_2 to Cocatalyst-Free Hydrogen Production. *ACS Catal.* **2019**, *9*, 345–364. [CrossRef]
7. Levinson, R.; Berdahl, P.; Akbari, H. Solar spectral optical properties of pigments-Part I: Model for deriving scattering and absorption coefficients from transmittance and reflectance measurements. *Sol. Energy Mater. Sol. Cells* **2005**, *89*, 319–349. [CrossRef]
8. Scanlon, D.O.; Dunnill, C.W.; Buckeridge, J.; Shevlin, S.A.; Logsdail, A.J.; Woodley, S.M.; Catlow, C.R.A.; Powell, M.J.; Palgrave, R.G.; Parkin, I.P.; et al. Band alignment of rutile and anatase TiO_2. *Nat. Mater.* **2013**, *12*, 798–801. [CrossRef]
9. Zhu, S.; Wang, D. Photocatalysis: Basic principles, diverse forms of implementations and emerging scientific opportunities. *Adv. Energy Mater.* **2017**, *7*, 1700841. [CrossRef]
10. Gao, Y.; Zhu, J.; An, H.; Yan, P.; Huang, B.; Chen, R.; Fan, F.; Li, C. Directly Probing Charge Separation at Interface of TiO_2 Phase Junction. *J. Phys. Chem. Lett.* **2017**, *8*, 1419–1423. [CrossRef]
11. Nosaka, Y.; Nosaka, A.Y. Generation and Detection of Reactive Oxygen Species in Photocatalysis. *Chem. Rev.* **2017**, *117*, 11302–11336. [CrossRef] [PubMed]
12. Yuan, W.; Cheng, L.; An, Y.; Lv, S.; Wu, H.; Fan, X.; Zhang, Y.; Guo, X.; Tang, J. Laminated Hybrid Junction of Sulfur-Doped TiO_2 and a Carbon Substrate Derived from Ti_3C_2 MXenes: Toward Highly Visible Light-Driven Photocatalytic Hydrogen Evolution. *Adv. Sci.* **2018**, *5*, 1700870. [CrossRef] [PubMed]
13. Chen, X.; Lou, Y.-B.; Samia, A.C.S.; Burda, C.; Gole, J.L. Formation of Oxynitride as the Photocatalytic Enhancing Site in Nitrogen-Doped Titania Nanocatalysts: Comparison to a Commercial Nanopowder. *Adv. Funct. Mater.* **2005**, *15*, 41–49. [CrossRef]
14. Asahi, R.; Morikawa, T.; Irie, H.; Ohwaki, T. Nitrogen-Doped Titanium Dioxide as Visible-Light-Sensitive Photocatalyst: Designs, Developments, and Prospects. *Chem. Rev.* **2014**, *114*, 9824–9852. [CrossRef] [PubMed]
15. Dong, F.; Zhao, W.; Wu, Z.; Guo, S. Band structure and visible light photocatalytic activity of multi-type nitrogen doped TiO_2 nanoparticles prepared by thermal decomposition. *J. Hazard. Mater.* **2009**, *162*, 763–770. [CrossRef]
16. Kong, X.; Peng, Z.; Jiang, R.; Jia, P.; Feng, J.; Yang, P.; Chi, Q.; Ye, W.; Xu, F.; Gao, P. Nanolayered Heterostructures of N-Doped TiO_2 and N-Doped Carbon for Hydrogen Evolution. *ACS Appl. Nano Mater.* **2020**, *3*, 1373–1381. [CrossRef]
17. Ansari, S.A.; Khan, M.M.; Ansari, M.O.; Cho, M.H. Nitrogen-doped titanium dioxide (N-doped TiO_2) for visible light photocatalysis. *New J. Chem.* **2016**, *40*, 3000–3009. [CrossRef]
18. Zeng, L.; Lu, Z.; Li, M.; Yang, J.; Song, W.; Zeng, D.; Xie, C. A modular calcination method to prepare modified N-doped TiO_2 nanoparticle with high photocatalytic activity. *Appl. Catal. B Environ.* **2016**, *183*, 308–316. [CrossRef]
19. Matsubara, K.; Danno, M.; Inoue, M.; Honda, Y.; Abe, T. Characterization of nitrogen-doped TiO_2 powder prepared by newly developed plasma-treatment system. *Chem. Eng. J.* **2012**, *181–182*, 754–760. [CrossRef]
20. Su, T.; Yang, Y.; Na, Y.; Fan, R.; Li, L.; Wei, L.; Yang, B.; Cao, W. An Insight into the Role of Oxygen Vacancy in Hydrogenated TiO_2 Nanocrystals in the Performance of Dye-Sensitized Solar Cells. *ACS Appl. Mater. Interfaces* **2015**, *7*, 3754–3763. [CrossRef]
21. Xu, Y.; Li, H.; Sun, B.; Qiao, P.; Ren, L.; Tian, G.; Jiang, B.; Pan, K.; Zhou, W. Surface oxygen vacancy defect-promoted electron-hole separation for porous defective ZnO hexagonal plates and enhanced solar-driven photocatalytic performance. *Chem. Eng. J.* **2020**, *379*, 122295. [CrossRef]
22. Huang, Y.; Yu, Y.; Yu, Y.; Zhang, B. Oxygen Vacancy Engineering in Photocatalysis. *Solar RRL* **2020**, *4*, 2000037. [CrossRef]
23. Wang, Z.; Lin, R.; Huo, Y.; Li, H.; Wang, L. Formation, Detection, and Function of Oxygen Vacancy in Metal Oxides for Solar Energy Conversion. *Adv. Funct. Mater.* **2022**, *32*, 2109503. [CrossRef]
24. Long, M.; Zheng, L. Engineering vacancies for solar photocatalytic applications. *Chin. J. Catal.* **2017**, *38*, 617–624. [CrossRef]
25. Cui, Z.; Xu, Y.; Xu, Y.; Zhao, M.; Li, S.; Wang, J.; Pan, D.; Wu, W. Effects of Solvent Treatment on the Formation of Oxygen Vacancy in TiO_2 via Vacuum Annealing. *J. Phys. Chem. C* **2022**, *126*, 21751–21758. [CrossRef]

26. Cui, Z.; Zhang, Z.; Tang, Z.; Nawfal Ghazzal, M.; Colbeau-Justin, C.; Shao, F.; Pan, D.; Wu, W. A facile strategy for the construction of visible light responsive P25 heterojunction via the annealing treatment with PEG. *Mater. Lett.* **2024**, *364*, 136325. [CrossRef]
27. Cui, Z.; Zhao, M.; Que, X.; Wang, J.; Xu, Y.; Ghazzal, M.N.; Colbeau-Justin, C.; Pan, D.; Wu, W. Facile Vacuum Annealing-Induced Modification of TiO_2 with an Enhanced Photocatalytic Performance. *ACS Omega* **2021**, *6*, 27121–27128. [CrossRef] [PubMed]
28. Cui, Z.; Zhao, M.; Li, S.; Wang, J.; Xu, Y.; Ghazzal, M.N.; Colbeau-Justin, C.; Pan, D.; Wu, W. Facile Vacuum Annealing of TiO_2 with Ethanol-Induced Enhancement of Its Photocatalytic Performance under Visible Light. *Ind. Eng. Chem. Res.* **2022**, *61*, 14455–14461. [CrossRef]
29. Bakre, P.V.; Tilve, S.G.; Shirsat, R.N. Influence of N sources on the photocatalytic activity of N-doped TiO_2. *Arab. J. Chem.* **2020**, *13*, 7637–7651. [CrossRef]
30. Jian, Y.; Chen, M.; Shi, J.; Shangguan, W. Preparations and photocatalytic hydrogen evolution of N-doped TiO_2 from urea and titanium tetrachloride. *Int. J. Hydrog. Energy* **2006**, *31*, 1326–1331.
31. Irie, H.; Washizuka, S.; Yoshino, N.; Hashimoto, K. Visible-light induced hydrophilicity on nitrogen-substituted titanium dioxide films. *Chem. Commun.* **2003**, 1298–1299. [CrossRef] [PubMed]
32. Batalović, K.; Bundaleski, N.; Radaković, J.; Abazović, N.; Mitrić, M.; Silva, R.A.; Savić, M.; Belošević-Čavor, J.; Rakočević, Z.; Rangel, C.M. Modification of N-doped TiO_2 photocatalysts using noble metals (Pt, Pd)—A combined XPS and DFT study. *Phys. Chem. Chem. Phys.* **2017**, *19*, 7062–7071. [CrossRef]
33. Wang, Y.; Chen, F.; Li, Y.; Lin, X.; Hu, H.; Yin, Q.; Hu, G. Novel synthesis of N-doped TiO_2 flower-like microspheres with excellent photocatalytic activity for removal of Cr(VI) and methylene blue. *Mater. Lett.* **2023**, *334*, 133745. [CrossRef]
34. Jaiswal, R.; Bharambe, J.; Patel, N.; Dashora, A.; Kothari, D.C.; Miotello, A. Copper and Nitrogen co-doped TiO_2 photocatalyst with enhanced optical absorption and catalytic activity. *Appl. Catal. B Environ.* **2015**, *168–169*, 333–341. [CrossRef]
35. Sathish, M.; Viswanathan, B.; Viswanath, R.P.; Gopinath, C.S. Synthesis, Characterization, Electronic Structure, and Photocatalytic Activity of Nitrogen-Doped TiO_2 Nanocatalyst. *Chem. Mater.* **2005**, *17*, 6349–6353. [CrossRef]
36. Zeng, L.; Lu, Z.; Yang, J.; Li, M.; Song, W.; Xie, C. Highly efficient visible-light driven photocatalyst with enhanced charge separation prepared by annealing continuously in ammonia and vacuum. *Appl. Catal. B Environ.* **2015**, *166–167*, 1–8. [CrossRef]
37. Li, C.; Wang, T.; Zhao, Z.-J.; Yang, W.; Li, J.-F.; Li, A.; Yang, Z.; Ozin, G.A.; Gong, J. Promoted Fixation of Molecular Nitrogen with Surface Oxygen Vacancies on Plasmon-Enhanced TiO_2 Photoelectrodes. *Angew. Chem. Int. Ed.* **2018**, *57*, 5278–5282. [CrossRef] [PubMed]
38. Elbanna, O.; Zhang, P.; Fujitsuka, M.; Majima, T. Facile preparation of nitrogen and fluorine codoped TiO_2 mesocrystal with visible light photocatalytic activity. *Appl. Catal. B Environ.* **2016**, *192*, 80–87. [CrossRef]
39. Katoh, R.; Furube, A.; Yamanaka, K.-I.; Morikawa, T. Charge Separation and Trapping in N-Doped TiO_2 Photocatalysts: A Time-Resolved Microwave Conductivity Study. *J. Phys. Chem. Lett.* **2010**, *1*, 3261–3265. [CrossRef]
40. Panepinto, A.; Cornil, D.; Guttmann, P.; Bittencourt, C.; Cornil, J.; Snyders, R. Fine Control of the Chemistry of Nitrogen Doping in TiO_2: A Joint Experimental and Theoretical Study. *J. Phys. Chem. C* **2020**, *124*, 17401–17412. [CrossRef]
41. Livraghi, S.; Paganini, M.C.; Giamello, E.; Selloni, A.; Di Valentin, C.; Pacchioni, G. Origin of Photoactivity of Nitrogen-Doped Titanium Dioxide under Visible Light. *J. Am. Chem. Soc.* **2006**, *128*, 15666–15671. [CrossRef] [PubMed]
42. Livraghi, S.; Elghniji, K.; Czoska, A.M.; Paganini, M.C.; Giamello, E.; Ksibi, M. Nitrogen-doped and nitrogen–fluorine-codoped titanium dioxide. Nature and concentration of the photoactive species and their role in determining the photocatalytic activity under visible light. *J. Photochem. Photobiol. A Chem.* **2009**, *205*, 93–97. [CrossRef]
43. Yang, G.D.; Jiang, Z.; Shi, H.H.; Xiao, T.C.; Yan, Z.F. Preparation of highly visible-light active N-doped TiO_2 photocatalyst. *J. Mater. Chem.* **2010**, *20*, 5301–5309. [CrossRef]
44. Wang, J.; Tafen, D.N.; Lewis, J.P.; Hong, Z.L.; Manivannan, A.; Zhi, M.J.; Li, M.; Wu, N.Q. Origin of photocatalytic activity of nitrogen-doped TiO_2 nanobelts. *J. Am. Chem. Soc.* **2009**, *131*, 12290–12297. [CrossRef] [PubMed]
45. Gai, L.G.; Duan, X.Q.; Jiang, H.H.; Mei, Q.H.; Zhou, G.W.; Tian, Y.; Liu, H. One-pot synthesis of nitrogen-doped TiO_2 nanorods with anatase/brookite structures and enhanced photocatalytic activity. *CrystEngComm* **2012**, *14*, 7662–7671. [CrossRef]
46. Saien, J.; Mesgari, Z. Photocatalytic degradation of methyl orange using hematoporphyrin/N-doped TiO_2 nanohybrids under visible light: Kinetics and energy consumption. *Appl. Organomet. Chem.* **2017**, *31*, e3755. [CrossRef]
47. Peng, Y.; Lo, S.; Ou, H.; Lai, S. Microwave-assisted hydrothermal synthesis of N-doped titanate nanotubes for visible-light-responsive photocatalysis. *J. Hazard. Mater.* **2010**, *183*, 754–758. [CrossRef] [PubMed]
48. Xiong, Z.H.; Chen, H.Y.; Lu, L.L.; Shan, R.; Zhang, Y.Y.; Yuan, H.R.; Chen, Y. Nitrogen-doped TiO_2/nitrogen-containing biochar composite catalyst as a photocatalytic material for the decontamination of aqueous organic pollutants. *ACS Omega* **2023**, *8*, 791–803. [CrossRef]
49. Zhou, X.S.; Peng, F.; Wang, H.J.; Yu, H.; Yang, J. Preparation of nitrogen doped TiO_2 photocatalyst by oxidation of titanium nitride with H_2O_2. *Mater. Res. Bull.* **2011**, *46*, 840–844. [CrossRef]